Creep induced tunnel collapse during construction – a case study of a mountain railway tunnel in Taiwan

Wen-Jie Shiu
Sinotech, Taipei, Taiwan

Fu-Yuan Hsiao
Sinotech, Taipei, Taiwan

Cheng-Hsien Tsai
Sinotech, Taipei, Taiwan

Shih-Hui Wang
Raito Engineering Corporation

ABSTRACT: The mountain railway No. 42 Tunnel once collapsed during construction when only the primary shotcrete lining was in place. According to geological analysis and excavation records, the major cause of disaster was presumably due to time-dependent behavior of rock. In order to elucidate the impact of creep-induced displacement during excavation, a simulation-based methodology, *i.e.* a viscoplastic model combining the two-component power model and the ubiquitous-joint model, is proposed. The time dependent parameters were calibrated using the back analysis from the convergence measurement data. The modelling results have illustrated that the excavation induced displacement can be dissociated into two parts, the instantaneous deformation due to stress relaxation, and the time dependent deformation due to creep. The overall study in terms of current findings has shown that our proposed model is a useful tool for investigating long term stability of tunnels surrounded by creep potential rock material.

Keywords: viscoplastic model, creep behavior, convergence, tunnel excavation.

1 INTRODUCTION

On September 28, 2015, the mountain railway No. 42 tunnel was affected by Typhoon Dujuan, and the traffic service was thus interrupted. The reconstruction plan of the tunnel was to move the original alignment toward the mountain side. During reconstruction, the side wall close to the 59K+160 mileage experienced circumferential cracks. Various structural support techniques were utilized to restrain rock deformation. Despite these efforts, the shotcrete continued to be squeezed and cracked, which eventually led to the collapse of the tunnel.

During excavation stage of mountain tunnels, the rock mass surrounding the tunnel will deform due to stress relaxation. It is necessary to implement appropriate support methods according to factors such as geological conditions, in-situ stress, rock mass strength, and construction methods to maintain the stability of the tunnel (Hsiao 2010). In addition to the above-mentioned reasons, the time-dependent deformation behavior of the rock mass has an impact on the long-term stability of the tunnel. For example, the Zhegu Mountain 317 Highway Tunnel located in Sichuan continues to exhibit significant surface cracking on its lining structure, even after more than a decade of operation.

Creep behavior of the surrounding metamorphic rock mass was presumed to be the cause of this phenomenon (Meng et al. 2013). Numerical simulations were extensively deployed to reveal tunnel mechanical behavior (Galli et al. 2003, Lorig & Varona 2013 and Barla & Barla 2000). This study attempts to use geological records and deformation monitoring data obtained from actual tunnel excavation to identify potential causes of this disaster. A numerical conceptual model based on finite difference FLAC3D model (Itasca 2014) is built-up to investigate the mechanism of tunnel close to the section where the collapse had occurred. The impact of time-dependent deformation of the surrounding rock on the long-term stability of the tunnel is also discussed in the present work.

2 GEOLOGICAL ANALYSIS AND EXCAVATION DATA

To investigate the cause and impact of the tunnel collapse event, we collected geological cross-section maps and relevant monitoring data along and near-by the collapse section to reveal the characteristics of the surrounding rock mass and excavation-induced deformation. Figure 1 gives the geological cross-section map of the tunnel from the section 59K+145 to 59K+175. The collapsed area in this event is located between 59K+154 and 59K+160, with a length of approximately 6 meters. According to the geological data shown in the diagram, the geological rock type in the section belongs to an interbedded shale and sandstone formation (N6). The results of the lab rock core uniaxial compression test show that this type of rock has a relatively low uniaxial compressive strength (UCS) of only about 1.97 MPa. The geological cross-section map reveals that the rock layers preceding and succeeding the collapse area exhibit shearing and comprise of mudstone. The boundary interfaces preceding the collapse have a northward tilt (N44-82E/38-58S), whereas those after the collapse have a southward tilt (N44-82E/38-58S), suggesting that the strata may have undergone folding, leading to the formation of fragile and brittle layers that could be one of the geological causes for the collapse.

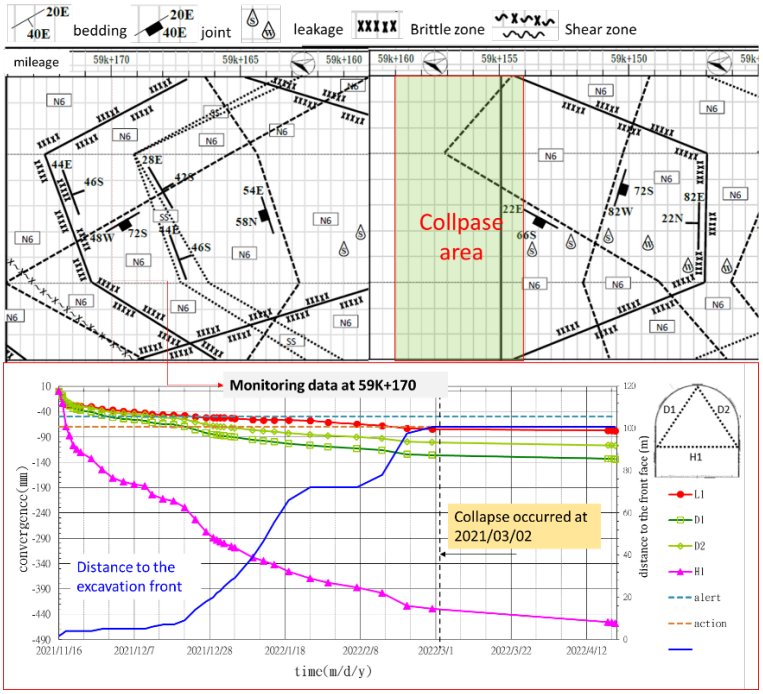

Figure 1. Geological map near the collapse section and convergence measurement data at 59K+170 mileage.

During tunnel reconstruction, various monitoring instruments were installed in accordance with the excavation advancement to observe the stability of the tunnel. The monitoring data near the collapse site (at 59k+170) displayed a substantial convergence of the rock mass, as depicted in Figure 1. It was noted that even after the excavation front moved over 100 meters away (which was 15 times the

diameter of the excavation), the convergence still continued to progress. The horizontal convergence was found to be approximately 430 mm.

3 METHODOLOGY

3.1 Creep model

This study utilizes the built-in Ubiquitous joint model (Ubi model) and Norton power law to simulate the instantaneous deformation and time-dependent creep behavior of tunnel excavation. The Ubiquitous joint model is an extension of the Mohr-Coulomb model, which incorporates one single set weak plane into the original Mohr-Coulomb element to simulate rock materials with bedding formation. Based on the geological map near the collapse section, different bedding orientation preceding and succeeding the collapse section were considered in the numerical model. The parameter settings were adopted from the geological cross-section provided in Figure 1. The first half of the tunnel was characterized by northward dipping bedding (N44-82E/38-58S), while southward dipping bedding (N44-82E/38-58S) was considered in the second half of the tunnel. Using this conceptual model, the influence of changes in bedding orientation on tunnel excavation deformation was investigated.

In general, when weak rock formations undergo time-dependent creep behavior, the primary creep with a faster strain rate occurs first, followed by the secondary creep with a slower strain rate. As shown in Figure 2, the two-component Norton power law divides the creep rate of the rock material into two regions according to the deviatoric stress applied to the rock mass. During the creep iteration, the creep rate behaves as the primary creep when the deviatoric stress is greater than a prescribed reference value (σ^{ref}). Otherwise, it enters the secondary creep stage. Each stage can be further controlled by a constant term A and a power law constant n to adjust the magnitude of creep deformation and the creep rate. The time-independent material parameters were adopted from the indoor testing of rock core samples, including uniaxial, triaxial, and direct shear tests (see Tables 1 and 2). The parameters for the visco-plastic materials are calibrated using the convergence measurement data from 59K+170 section and the relevant parameters are summarized in Table 3.

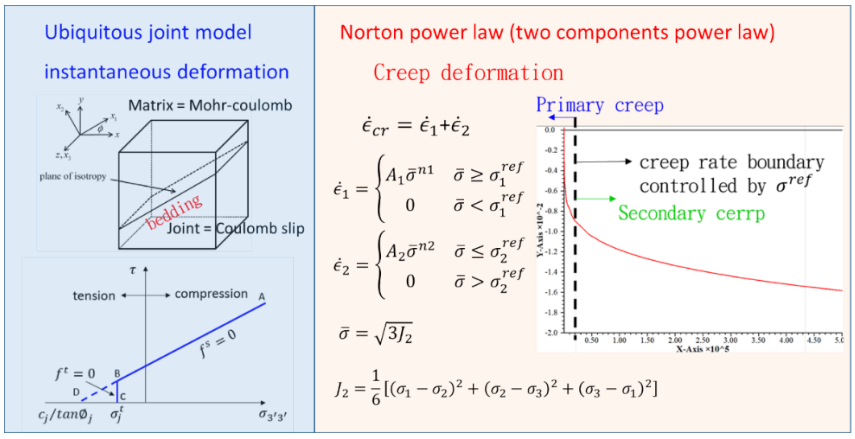

Figure 2. Constitutive model used for bedding material.

Table 1. Rock matrix property.

Rock formation		N4	N5	N6	N7	N8
Young's modulus	[GPa]	1.5	3.75	0.2	1.5	1.5
UCS	[MPa]	13.5	54	0.2	13.5	13.5
Cohesion	[MPa]	2.46	9.83	0.41	2.46	2.46
Friction angle	[°]	38	38	35	38	38

Table 2. Bedding property.

Beddings		preceding the collapse	succeeding the collapse
Orientation	[-]	N80°W/22°N	N60°E/42°S
Cohesion	[MPa]	0.041	0.041
Friction angle	[°]	30	30

Table 3. Property for creep material.

Rock formation		N6 formation	Other formations
A_1	[-]	$9x10^{-46}$	$5x10^{-48}$
A_2	[-]	$1.5x10^{-46}$	$5x10^{-48}$
n_1	[-]	6.625	6.05
n_2	[-]	6.525	5.85
σ^{ref}	[MPa]	0.3	0.3

3.2 Model geometry and boundary conditions

The No. 42 tunnel has an inverted D-shaped cross-section (Figure 3). The tunnel diameter is 5.6 m, and the shotcrete thickness is 15 cm. To prevent boundary effects, the model dimension was set to 100 m high and 100 m wide, with a tunnel length of 30 m. The axial line of the tunnel was represented as a curved line, as shown in Figure 3, to more accurately reflect the actual linear variation in the collapse section of the tunnel. Based on the geological profile data, the strata encountered by tunnel No. 42 near the collapse section can be divided into five rock types from bottom to top: N4, N5, N6, N7, and N8. This geological stratification was also accounted for in the numerical model. Boundary conditions were set such that stress boundaries are used on the upper and right boundaries (mountain side), while displacement boundaries (roller boundaries) are set on the remaining boundaries. Since the upper boundary in the model does not represent the actual ground surface, the corresponding overburden stress is set on the upper boundary.

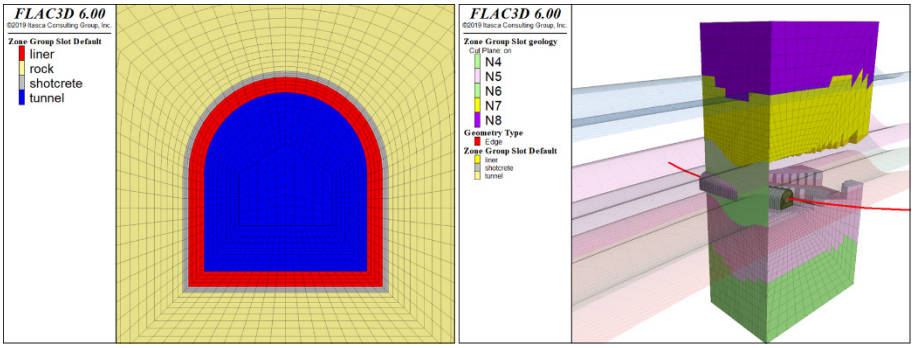

Figure 3. Tunnel cross section (left) and model geometry (right).

4 RESULTS AND DISCUSSION

Figure 4 gives the rock displacement trend observed at different excavation stages. The yellow dot marked in the figure denotes the middle cross section of the model. The modeling results obtained from this section were compared with the actual convergence data measured at the section 59K+170. It should be noted that most of the tunnel alignment belongs to the N6 weak rock formation, while only a few areas of the invert being N5 harder rock formation. At the 4th excavation stage, most of the rock displacement was observed on the tunnel crown and sidewalls, with minor deformation on the invert. This phenomenon is likely related to the spatial distribution of rock mass types. When excavation advancement progresses, the amount of rock displacement gradually increases. In terms of the overall rock displacement trend, the most significant displacement occurs in the middle section

of the model (*i.e.,* the tunnel collapse section) where the increase in displacement is mainly produced in the tunnel crown and sidewalls. The maximum displacement of the surrounding rock exceeds 60 cm. This section is located approximately at the turning point where the bedding orientation changes from originally dipping northwards to dipping southwards, forming a folded structure. The tunnel excavation stimulates the development of rock deformation as it passes through this structure, which is detrimental to the stability of the tunnel.

It can be seen from the convergence history measured in the middle section that the convergence increases drastically when the excavation front approaches and passes the monitoring section. The increasing trend of convergence can be divided into two parts: the first part is from the beginning of excavation to the excavation face approaching and passing the monitoring section. The rock displacement in this stage increases significantly. It is presumed that the displacement increment at this time is mostly due to the instantaneous deformation caused by the rock mass stress relaxation; the second part is when the excavation front moves away from the monitoring section. At this time, the rock mass at the monitoring section has approached or reached a state of complete decompression. However, the convergence continues to increase. This corresponds to a typical time-dependent creep behavior. After the tunnel excavation is completed, the model predicts a horizontal convergence (H1) of approximately 80 cm (Figure 10) and the tunnel crown settlement (L1) exceeds 40 cm. We further compared those findings with the field measured values and found out that the measured H1 and L1 were 42 cm and 8.5 cm respectively, which were smaller than the modeling predictions. This difference is mainly related to the timing of installation and measurement of monitoring instruments. In the numerical simulation, the monitoring points can be set in advance in the unexcavated rock mass, so the rock displacement presented by the numerical simulation includes the complete deformation of the rock mass from the initial stress to the complete stress relaxation. However, in the real tunnel excavation process, measuring instruments can only be installed after the excavation front passes through the monitoring section. This implies that the monitoring section has been decompressed to a considerable extent, so the measured value represents only part of the deformation caused by the relaxation of the current in-situ stress. It is reasonable that the measured convergence data is less than the numerical predictions. To allow the fair comparison between the two data, we could remove the deformation that has occurred before the excavation passes through the monitoring section. According to the in-situ measurement data, the distance between the tunnel excavation front and the monitoring section (at 56K+170) is 1.68 m. Thus, the amount of deformation that cannot be measured due to the limitation of the initial measurement timing is removed from the numerical model. By doing so, the deducted model results reasonably fit the measured convergence data (Figure 5).

Figure 5 shows the displacement contour of the overall model after tunnel excavation. The majority of rock was produced in the N6 rock formation and the displacement magnitude of the mountain side is greater than that of the river side. It is worthwhile to mention that the rock displacement does not extend to the upper model boundary. This implies that the tunnel collapse event might have less impact on the slope deformation above it.

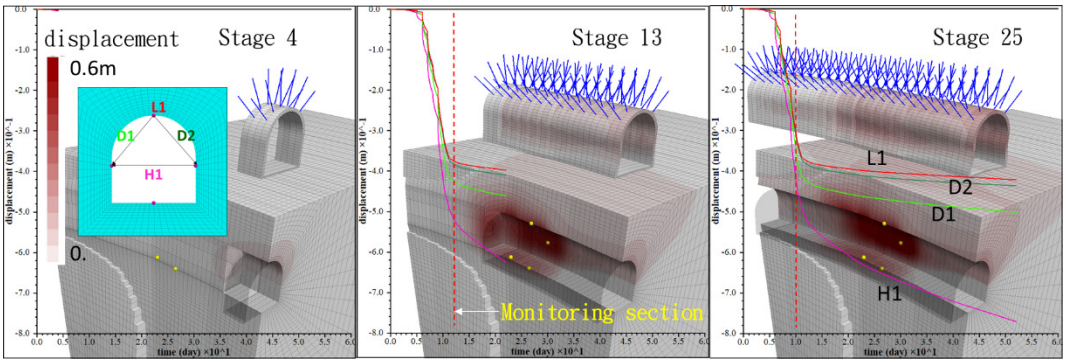

Figure 4. Rock displacement contour and convergence history in the middle cross section.

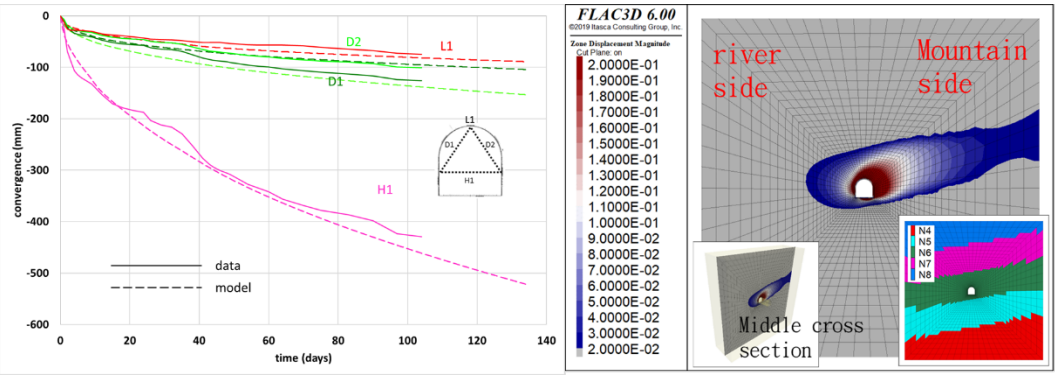

Figure 5. Rock displacement contour and convergence history in the middle cross section.

5 CONCLUSION

The reconstruction of the No. 42 tunnel was planned to shift the tunnel alignment from its original position toward the mountain side. During reconstruction, a part of tunnel was surrounded by weak and fractured rock formation, resulting in considerable sidewall deformation during excavation. The time dependent rock displacement behavior was presumed to be the main cause leading to the eventual tunnel collapse. In order to reveal the mechanism of the tunnel collapse event, we propose a three-dimensional finite difference numerical model using Ubiquitous joint model (Ubi model) combining Norton power law to simulate the instantaneous rock deformation as well as time-dependent creep behavior of tunnel excavation. The spatial rock formation distribution was also accounted for in the model. The rock mass properties were adopted from the lab test of the rock core samples and the in-situ convergence measurement data. Numerical results show that instantaneous decompression deformation first occurs in the initial stage of tunnel excavation, and then the creep induced deformation comes later. By removing the rock displacements that were produced before installation of monitoring sensors from the numerical model, the model results were aligned with the measured data in terms of the convergence evolution near the collapse section. Nevertheless, the rock displacement were mainly produced within the N6 rock formation close to the altitude of the tunnel and had a limited impact on the slope deformation above it. For the time-dependent creep behavior of the rock mass, the continuous and slow deformation of the surrounding rock will have a certain impact on the lining structure. It is recommended that the permanent lining in the collapsed section be appropriately thickened or stiffened to ensure the long term stability and safety.

REFERENCES

Hsiao, F.Y. 2010. *Deformation prediction and support countermeasurement in the intersection of mountain tunnel*. Ph.D. thesis. National Cheng Kung University, Taiwan.

Meng, J.B., Li, T.B., Kiang, Y., Wang, R., & Li, Y. 2013. *Characteristics and mechanisms of large deformation in the Zhegu mountain tunnel on the Sichuan-Tibet highway*. *Tunnelling and Underground Space Technology*, Vol. 37, pp. 157-164.

Galli, G., Grimaldi, A., and Leonardi, A. 2004. *Three-dimensional modelling of tunnel excavation and lining*. *Computers and Geotechnics*, Vol. 31, Issue 3, pp. 171-183.

Lorig, L.J., Varona, P. 2013. *Guidelines for numerical modelling of rock support for mines*. *Proceedings of the Seventh International Symposium on Ground Support in Mining and Underground Construction*, Australian Centre for Geomechanics

Barla, G., and Barla, M. 2000. *Continuum and discontinuum modelling in tunnel engineering*. *Rudarsko-geolosko-naftni zbornik*, Vol. 12, pp. 45-57.

Itasca Consultants Group, ICG. 2014. *Fast Lagrangian Analysis of Continua in 3 Dimensions* user manual.